Role of checkpoint kinase 1 (Chk1) in the mechanisms of resistance to histone deacetylase inhibitors

Ju-Hee Lee, Megan L. Choy, Lang Ngo, Gisela Venta-Perez, and Paul A. Marks[1]

Cell Biology Program, Sloan-Kettering Institute, Memorial Sloan-Kettering Cancer Center, New York, NY 10065

Histone deacetylase inhibitors (HDACi) are a new group of anticancer drugs with tumor selective toxicity. Normal cells are relatively resistant to HDACi-induced cell death compared with cancer cells. Previously, we found that vorinostat induces DNA breaks in normal and transformed cells, which normal but not cancer cells can repair. In this study, we found that checkpoint kinase 1 (Chk1), a component of the G2 DNA damage checkpoint, is important in the resistance of normal cells to HDACi in vitro and in vivo. Inhibition of Chk1 activity with Chk1 inhibitor (UCN-01, AZD7762, or CHIR-124) in normal cells increases their sensitivity to HDACi (vorinostat, romidepsin, or entinostat) induced cell death, associated with extensive mitotic disruption. Mitotic abnormalities included loss of sister chromatid cohesion and chromosomal disruption. Inhibition of Chk1 did increase HDACi-induced cell death of transformed cells. Thus, Chk1 is an important factor in the resistance of normal cells, and some transformed cells, to HDACi-induced cell death. Use of Chk1 inhibitors in combination with anticancer agents to treat cancers may be associated with substantial toxicity.

checkpoint kinase 2 | γH2AX | histone deacetylases

Histone deacetylase inhibitors (HDACi) are a new class of selective anticancer agents that inhibit zinc-dependent histone deacetylases (HDACs) (1, 2). Two HDACi, vorinostat and romidepsin, are approved by the Food and Drug Administration (FDA) for the treatment of cutaneous T-cell lymphoma (3–5). These HDACi, as well as about two dozen other HDACi are in clinical trials, generally in combination therapy, for both hematologic and solid neoplasms (1, 2, 6, 7).

In man, there are 11 zinc-dependent HDACs classified on the basis of homology to yeast: class I (HDACs 1, 2, 3, and 8), class IIa (HDACs 4, 5, 7, and 9), class IIb (HDACs 6 and 10), and class IV (HDAC11) (2). The biological roles of the HDACs in man are not completely understood. They are not redundant in their activities. There are 3,600 acetylated lysine sites in 1,750 proteins. Only ~10% of these lysine acetylation sites are altered by vorinostat (8). HDACs are involved in regulation of gene expression by changing chromatin structure. In addition, HDACi have nonhistone protein substrates, which have a role in many cell pathways, including cell cycle progression, cell migration, apoptosis, and angiogenesis (2, 6). Acetylation of these proteins may alter their function in regulating these pathways.

Normal cells are relatively resistant to vorinostat and related HDACi, a fact not well understood (9). We previously showed that vorinostat induces DNA damage in both transformed and normal cells. Normal cells can repair the DNA damage, whereas transformed cells cannot and undergo apoptosis and death (10).

The G2 checkpoint is a cellular activity response to DNA damage. A genomewide analysis identified the G2 checkpoint as a coordinated action of proteins involved in DNA repair, DNA replication, cell cycle control, chromatin regulation, and RNA processing (11). Chk1 is a protein kinase that is a critical component of the G2 checkpoint, arresting cell cycle progression from G2 phase to mitosis in response to DNA damage (11–15). Many transformed cells have a defect in the G2 checkpoint that gives them a survival benefit (12, 16). Inhibition

of Chk1 in the absence of DNA damage does not induce somatic cell death (16).

Chk1 has been considered a good target for drugs to increase the therapeutic effectiveness of anticancer agents (13, 15, 17–26). UCN-01, 7-hydroxystaurosporine, is an inhibitor of Chk1, which has been in clinical trials in patients with neoplasms (22–24). Two other Chk1 inhibitors, AZD7762 (5-(3-Fluorophenyl)-3-ureidothiophene-N-[(S)-piperidin-3-yl]-2-carboxamide) and CHIR-124 ((S)-3-(1H-benzo[d]imidazol-2-yl)-6-chloro-4-(quinuclidin-3-ylamino)quinolin-2(1H)-one) are in earlier stages of development as potential anticancer agents (19, 20).

In this study, we show that inhibition of Chk1 makes normal cells (human foreskin fibroblast, HFS) sensitive to HDACi-induced cell death. Chk1 inhibitor also enhanced HDACi-induced transformed cell death. We found that vorinostat induces chromosomal abnormalities. HFS cells, but neither human prostate cancer (LNCaP) nor human lung adenocarcinoma (A549) cells, can recover from the HDACi-induced chromosomal abnormalities. In transformed cells, the HDACi caused a failure of sister chromatid cohesion. UCN-01, AZD7762, or CHIR-124 inhibits Chk1 enzyme activity and suppresses accumulation of Chk1 protein in both normal and transformed cells. None of the Chk1 inhibitors significantly inhibited Chk2 enzyme activity. In vivo studies, we show that administration of UCN-01 plus vorinostat to normal adult mice is toxic. It causes chromosomal abnormalities in bone marrow cells similar to that observed in the in vitro cell culture studies. The present findings indicate that Chk1 accounts, in part at least, for the relative resistance of normal cells to HDACi and may contribute to resistance of transformed cells to HDACi. These findings suggest that clinical trials with Chk1 inhibitor in combination with a DNA damaging agent, such as HDACi, may enhance anticancer activity, but can be associated with substantial toxicity.

Results

Inhibiting Chk1 Potentiates HDACi-Induced Cell Death in Normal and Transformed Cells. HDACi, vorinostat (suberoylanilide hydroxamic acid), romidepsin (depsipeptide), or entinostat (MS-275), at concentrations that induce transformed cell (LNCaP and A549) death do not induce normal cell death (HFS) (Fig. 1). Vorinostat induces DNA double strand breaks (DSBs) in both normal and transformed cells (10). Normal, but not transformed cells can repair the DNA damage. To gain insight into the mechanisms of

Fig. 1. Inhibitors of Chk1 enhance HDACi-induced cell death in normal cells (HFS) and transformed cells (LNCaP and A549). Cell viability of (*A*) HFS, (*B*) LNCaP, and (*C*) A549 cells cultured with vorinostat (V), UCN-01 (U), both inhibitors (V + U), or without inhibitor (control) for 72 h. Cell viability of (*D*) HFS, (*E*) LNCaP, and (*F*) A549 cells cultured with entinostat (Enti), UCN-01 (U), entinostat plus UCN-01 (Enti + U), romidepsin (Romi), romidepsin plus UCN-01 (Romi + U), or without inhibitor (control). Cell viability of (*G*) HFS, (*H*) LNCaP, and (*I*) A549 cells cultured with vorinostat (V), AZD7762 (AZD), and with both inhibitors (AZD + V), CHIR-124 (CHIR), and with both inhibitors (CHIR + V). Cell viability was determined as previously described (10). Data are represented as mean ± SD. ***P < 0.001. P value was derived from the two-way ANOVA.

resistance of normal cells to HDACi, we determined whether Chk1, a critical component of the G2 DNA damage checkpoint, protects normal cells (HFS) from HDACi-induced cell death. Normal HFS and transformed cells, LNCaP and A549, were cultured with the HDACi, 5 μM of vorinostat, 5 nM romidepsin, or 2 μM entinostat alone and in combination with 400 nM UCN-01. Vorinostat or UCN-01 alone caused no detectable loss of HFS viability (Fig. 1*A*). Vorinostat plus UCN-01 caused about 60% cell death of HFS cells (Fig. 1*A*). Vorinostat plus UCN-01 caused a significant increase in LNCaP and A549 cell death compared with vorinostat alone (Fig. 1 *B* and *C*).

We next determined the effect of a combination of Chk1 inhibitor with two other HDACi. Romidepsin plus UCN-01 caused 100% loss in HFS viability by 72 h compared with 20–30% for either inhibitor alone (Fig. 1*D*). Romidepsin plus UCN-01 increased A549 but not LNCaP cell death compared with either inhibitor alone (Fig. 1 *E* and *F*). Entinostat plus UCN-01 caused 100% loss in HFS viability by 72 h, comparable to romidepsin (Fig. 1*D*). Entinostat plus UCN-01 increased cell death of A549 but not LNCaP (Fig. 1 *E* and *F*). These results indicate that in cells cultured with HDACi, inhibiting Chk1 can cause cell death of normal cells and enhance cell death of transformed cells, which are resistant to HDACi.

Vorinostat inhibits HDACs 1, 2, 3, and 6; romidepsin inhibits primarily HDAC1; and entinostat inhibits HDACs 1, 2, and 3 (27). These findings suggest that inhibition of class I HDACs, HDAC1 in particular, plays a role in UCN-01 inducing normal and transformed cell death in combination with HDACi. Differences in the molecular abnormalities between LNCaP and A549 cells may account for the differences in sensitivity of these transformed cells to Chk1 inhibition (28).

Further, we examined the effect of two other Chk1 inhibitors, AZD7762 and CHIR-124 on the sensitivity of HFS, LNCaP, and A549 cells to the HDACi. Each of these Chk1 inhibitors at 2 μM made the normal cells (HFS) sensitive to HDACi-induced cell death. Neither alone induced HFS cell death (Fig. 1*G*).

AZD7762 and CHIR-124 increased HDACi-induced cell death of A549 but not LNCaP (Fig. 1 *H* and *I*).

Combination of UCN-01 Plus Vorinostat Decreases Chk1 Enzyme Activity and Chk1 Protein Levels in Normal (HFS) and Transformed Cells (LNCaP and A549). We next showed that UCN-01 inhibited Chk1 enzyme activity and suppressed Chk1 protein level in normal and transformed cells (Fig. 2). Culture with 5 μM vorinostat did not decrease Chk1 kinase activity in HFS (Fig. 2*A*) or LNCaP (Fig. 2*B*). Culture of HFS (Fig. 2*A*) or LNCaP (Fig. 2*B*) with 400 nM UCN-01 plus vorinostat significantly inhibited Chk1 kinase activity compared with either inhibitor alone. In A549 cells (Fig. 2*C*), vorinostat alone, or in combination with 400 nM UCN-01 inhibited Chk1 kinase activity 50 and 75%, respectively. UCN-01 did not inhibit Chk2 enzyme activity in HFS or A549 (Fig. 2 *D* and *F*). The Chk1 inhibitors, AZD7762 and CHIR-124, at 1 μM caused a decrease in Chk1 kinase activity but not in Chk2 kinase activity in HFS and LNCaP (Fig. 2 *D* and *E*). A549 cells cultured with 2 μM AZD7762 caused 80% inhibition of Chk1 kinase activity, but no inhibition of Chk2 activity. A total of 2 μM CHIR-124 caused 40 and 50% inhibition of both Chk1 and Chk2 kinase activity in A549 cells, respectively (Fig. 2*F*).

Chk1 protein level was assayed in HFS, LNCaP, and A549 cells cultured with UCN-01, vorinostat, or a combination of both inhibitors for 24 h. Vorinostat caused a decrease in Chk1 protein levels in HFS, LNCaP, and A549 cells. The combination of vorinostat plus UCN-01 caused a greater decrease in levels of Chk1 protein in both normal and transformed cells than vorinostat alone (Fig. 2 *G* and *H*). There was no change in Chk2 protein levels in HFS, LNCaP, and A549 cells.
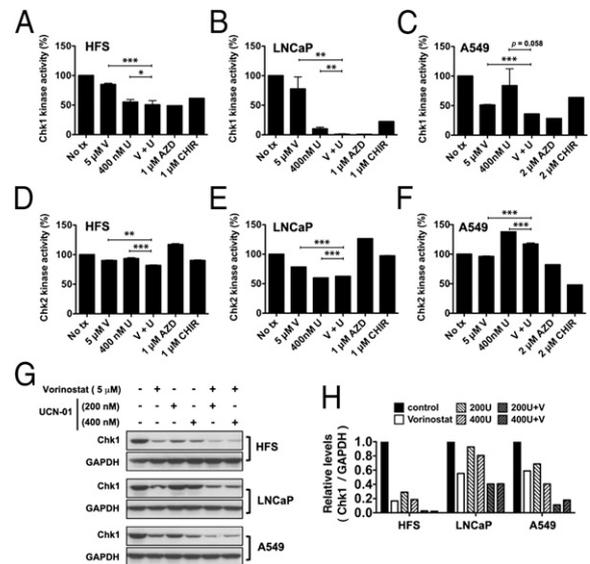

Fig. 2. Combination of vorinostat plus UCN-01 decreases Chk1 enzyme activity and protein level in HFS, LNCaP, and A549 cells. Chk1 enzyme activity in (*A*) HFS, (*B*) LNCaP, and (*C*) A549 cells cultured with indicated additions for 24 h: vorinostat (V), UCN-01 (U), vorinostat plus UCN-01 (V + U), AZD7762 (AZD), and CHIR-124 (CHIR). Chk2 enzyme activity in (*D*) HFS, (*E*) LNCaP, and (*F*) A549 cells cultured with indicated additions for 24 h: vorinostat (V), UCN-01 (U), vorinostat plus UCN-01 (V + U), AZD7762 (AZD), and CHIR-124 (CHIR). Cell lysates immunoprecipitated with Chk1 or Chk2 antibody (EMD4Biosciences) and analyzed by K-Lisa (31). Data are represented as mean ± SD. *P < 0.05, **P < 0.01, ***P < 0.001. P value was derived from the two-tailed Student's *t* test. (*G*) Immunoblot of Chk1 in HFS, LNCaP, and A549 cells cultured with indicated inhibitors for 24 h. GAPDH is a loading control. (*H*) Quantification of Chk1 protein levels. Graphs expressed as a ratio to the loading control of the levels of Chk1.

To verify the increased normal cell death in culture with HDACi plus Chk1 inhibition, we used shRNA to knockdown Chk1 in HFS cells. Knockdown of Chk1 by shRNA did not affect cell viability and cell growth (Fig. S1*A*). Chk1 knockdown of normal cells cultured with 5 μM vorinostat for up to 96 h resulted in 30% cell death compared with Chk1 knockdown of normal cells without inhibitor (Fig. S1). Taken together, these data indicate that chemical inhibition of Chk1 activity sensitized HFS cells to vorinostat to a greater extent than knockdown of Chk1.

Inhibition of Chk1 Increases the Accumulation of DNA DSBs Induced by Vorinostat in Normal and Transformed Cells. Chk1 inhibition with UCN-01 increased DNA DSBs, as indicated by the accumulation of phosphorylated H2AX (γH2AX), in HFS, LNCaP, and A549 cells cultured with 5 μM vorinostat compared with cells cultured with HDACi alone (Fig. 3*A*). The accumulation of DNA damage is increased by knockdown of Chk1 in normal cells compared with scramble shRNA transfected normal cells (Fig. S1*C*). There was no increase in the accumulation of γH2AX in Chk1 knockdown of HFS cells cultured with vorinostat.

To quantify the accumulation of DNA DSBs in normal and transformed cells, comet assays were performed with HFS (Fig. 3*B*) and LNCaP cells (Fig. 3*C*) after culture with 400 nM UCN-01, 5 μM vorinostat, or both inhibitors. There were significantly increased levels of DNA damage in HFS cells cultured in UCN-01 plus vorinostat compared with cells cultured with HDACi alone (Fig. 3*D*). In LNCaP, there was no significant difference in comet tail values in cells cultured with vorinostat or UCN-01 alone and cells cultured with both agents (Fig. 3*E*).
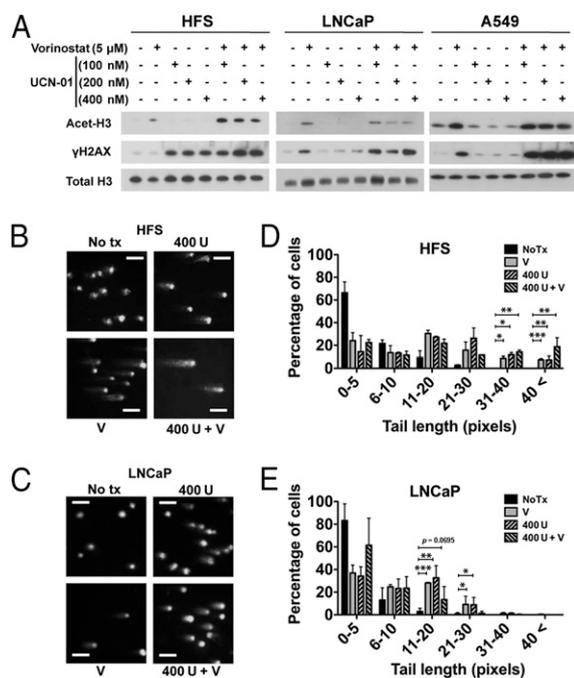
Fig. 3. Inhibition of Chk1 increases HDACi-induced accumulation of γH2AX. (*A*) Immunoblots of acetylated histones H3 (Acet-H3) and γH2AX of HFS, LNCaP, and A549 cells cultured for 24 h with indicated inhibitors. Histone H3 is a loading control. Representative images of neutral comet assay of (*B*) HFS and (*C*) LNCaP cells at 24 h of culture with indicated inhibitors: 5 μM vorinostat (V), 400 nM UCN-01 (U), vorinostat plus UCN-01 (V + U). (Scale bar, 100 μm.) Percentages of cells with a given comet tail length of (*D*) HFS and (*E*) LNCaP cells cultured with indicated inhibitors. Data are represented as mean ± SD. *P < 0.05, **P < 0.01, ***P < 0.001. P value was derived from the two-tailed Student's t test.

Vorinostat, UCN-01, and a Combination of Both Inhibitors Induce Chromosome Abnormalities in Normal and Transformed Cells. We next examined mitotic spreads prepared from cells in culture with vorinostat or UCN-01 and with both inhibitors for 24 h. HFS cells cultured with 5 μM vorinostat for 24 h exhibited a block in mitotic entry (Fig. 4*A*). In HFS cultured with 400 nM UCN-01 or with 400 nM UCN-01 plus 5 μM vorinostat, there was pulverization of chromosomes (Fig. 4*A*). LNCaP cells cultured with 5 μM vorinostat for 24 h showed a failure of sister chromatid cohesion and accumulation of chromosomal breaks and pulverization (Fig. 4 *B* and *D*). LNCaP in culture with 400 nM UCN-01 or a combination of UCN-01 plus 5 μM vorinostat exhibited more extensive chromosomal breaks than cells cultured with HDACi (Fig. 4 *B* and *D*). Metaphase spreads of A549 cells cultured with 400 nM UCN-01 or a combination of UCN-01 with 5 μM vorinostat exhibited predominantly chromosomal breaks and pulverization (Fig. 4 *C* and *D*).

The average number of chromosomal breaks per metaphase was higher in both LNCaP and A549 cells cultured with a combination of vorinostat plus UCN-01 than vorinostat or UCN-01 alone (Fig. 4*E*). These results indicate that vorinostat induces DNA DSBs and blocks chromatid cohesion in transformed cells. The inhibition of Chk1 increases accumulation of chromosomal abnormalities in normal and transformed cells.

To further examine whether vorinostat induces a block of mitotic entry, we determined the level of phosphorylated histone H3 (p-H3), a marker of mitotic entry. In LNCaP cells, and to a lesser extent in A549 cells, the level of p-H3 was increased by vorinostat, but not in normal cells (HFS) (Fig. 4*F*). These findings indicate that vorinostat increases a block at entry into mitosis in HFS, which presumably prevents normal cell death. Inhibition of Chk1 in HFS cells cultured with vorinostat results in accumulation of chromosomal abnormalities (Fig. 4*A*) and cell death (Fig. 1). Transformed cells, which have a defective G2 checkpoint, cultured with HDACi enter mitosis and accumulate chromosomal abnormalities with consequent cell death. Chk1 inhibition in LNCaP and A549 cells cultured with HDACi increases abnormal chromosomes (Fig. 4 *B* and *C*) and increases transformed cell death (Fig. 1).

We found that normal but not transformed cells can repair chromosomal breaks induced by vorinostat. After 24 h in culture with 5 μM vorinostat, HFS and LNCaP cells were transferred to inhibitor-free medium. Chromosomal breaks persisted in LNCaP cells but not in HFS cells (Fig. 4*G*). These findings are consistent with our previous observation that DNA DSBs induced by vorinostat persist in transformed, but not normal cells, even after removal of vorinostat (10).

Vorinostat inhibits HFS and LNCaP cell growth. To determine whether cells can recover and proliferate after 72 h in culture with vorinostat or UCN-01 alone or in combination, cells were placed in culture without inhibitors. HFS cells began proliferating within 36–48 h, whereas LNCaP cells did not recover capacity to proliferate in culture for up to 96 h (Fig. 4*H*).

UCN-01 Plus HDACi Is Toxic to Normal Mice. UCN-01 as monotherapy and in combination with anticancer drugs has been studied in clinical trials in patients with cancer (22–25). The effect of administering a combination of HDACi with UCN-01 to normal mice is not known. B6D2F1 normal adult mice were given 10 mg/kg UCN-01 alone or with 50 mg/kg vorinostat intraperitoneally daily for 5 d. Previous studies showed that 50 mg/kg vorinostat is well tolerated in mice (29). No weight loss occurred in mice administered vorinostat (Fig. 5*A*). Mice administered 10 mg/kg UCN-01 or both 10 mg/kg UCN-01 and 50 mg/kg vorinostat had an average weight loss of 8.3% or 15.8% of initial body weight, respectively, by day 5 of treatment (Fig. 5*A*). One mouse, which received both inhibitors, died on day 5.
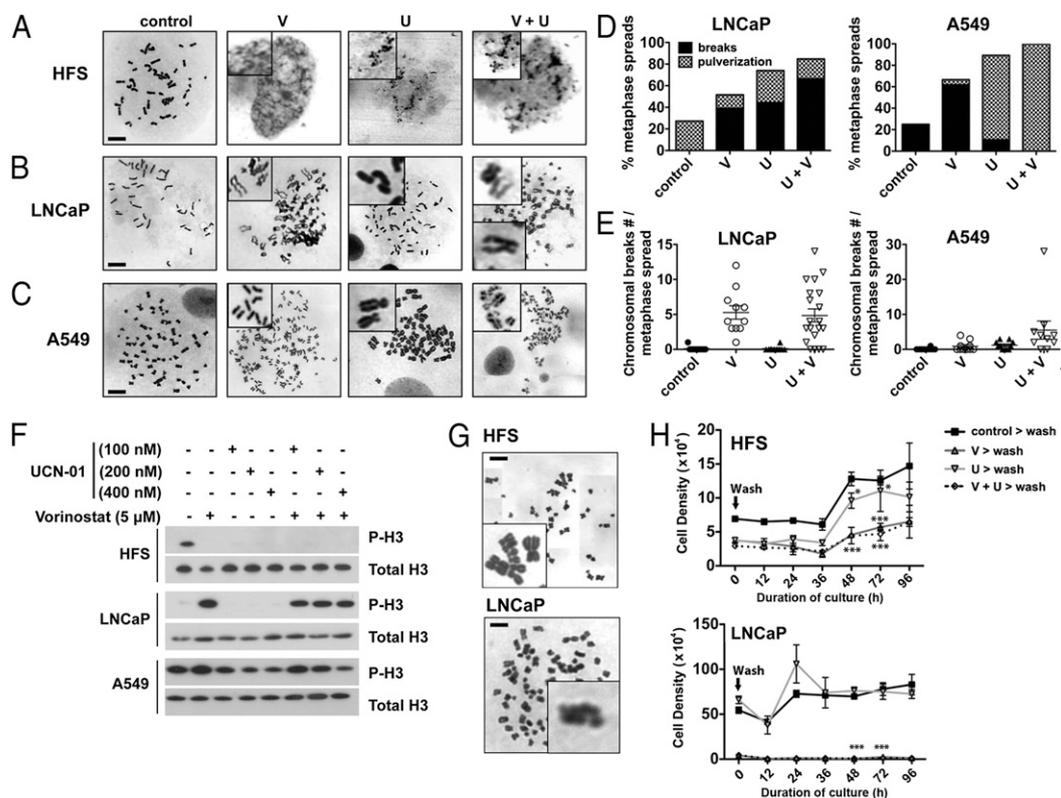
Fig. 4. Vorinostat, UCN-01, and in combination induce abnormal mitosis. Representative mitotic spreads of (*A*) HFS, (*B*) LNCaP, and (*C*) A549 cells in 24 h culture without (control) or with indicated inhibitors: 5 μM vorinostat (V), 400 nM UCN-01 (U), vorinostat plus UCN-01 (V + U). (Scale bar, 10 μm.) (*D*) Percentage of metaphase spreads with the indicated aberration in LNCaP and A549 cells cultured with indicated inhibitors (*n* > 150 cells). (*E*) Aberrations per metaphase in LNCaP and A549 cells cultured with indicated inhibitor. (*F*) Immunoblots of phosphorylated H3 (p-H3) of HFS, LNCaP, and A549 cells cultured with indicated inhibitors for 24 h. Histone H3 is a loading control. (*G*) Representative mitotic spreads HFS and LNCaP cells cultured with vorinostat for 24 h followed by 24 h cultured without inhibitor. (Scale bar, 10 μm.) (*H*) Cell density in cultures of HFS and LNCaP for 72 h with indicated inhibitors, then cultured without inhibitors for indicated times. "0 h" is time of medium replacement at 72 h. Viable cells were measured by trypan blue staining. Data are represented as mean ± SD. *$P < 0.05$, ***$P < 0.001$. P value was derived from two-way ANOVA.

Mitotic chromosome analysis of bone marrow cells was performed on mice that received vorinostat plus UCN-01 or each inhibitor alone and control mice that received vehicle. Chromosome breaks and failure of sister chromatid cohesion were observed in bone marrow cells from mice that received either 50 mg/kg vorinostat or 10 mg/kg UCN-01. Mice receiving vorinostat plus 10 mg/kg UCN-01 displayed massive disruption of chromosome structure (Fig. 5 *B* and *C*).

Pathological studies of autopsied mice that received 50 mg/kg vorinostat plus 10 mg/kg UCN-01 showed bleeding in the gastrointestinal tract, shrinkage of spleen, and depletion of bone marrow. There was depletion of white pulp and red pulp as well as hemorrhaging in spleen, which were more severe than in spleen of mice receiving vorinostat or UCN-01 alone (Fig. S2). Metabolic abnormalities were present in mice that received vorinostat plus UCN-01, including hyperglycemia. This has been reported in patients receiving UCN-01 in clinical trials (22). Taken together, the present data suggest that a combination of vorinostat plus UCN-01 is toxic to normal cells both in vivo and in vitro.

Discussion

These studies show that Chk1, a critical component of the G2 DNA damage response (11, 13–16), protects normal cells from HDAC inhibitor-induced cell death. Chk1 plays a crucial role in the ability of normal cells to recover from vorinostat-induced DNA double strand breaks. Most transformed cells have a defective Chk1, G2 damage response, as evidenced by the fact that

transformed cells continue to enter mitosis in the presence of DNA damage, which can lead to apoptosis and cell death. The intact Chk1 in normal cells, in part at least, accounts for the relative resistance of normal cells to HDAC inhibitor-induced cell death (9, 10).

We found that inhibitors of Chk1 (UCN-01, AZD7762, and CHIR-124) administered with the DNA damaging drug, an HDACi (vorinostat, romidepsin, or entinostat) induced normal cell death both in vitro (cell cultures) and in vivo (normal adult mice). The Chk1 inhibitors can enhance HDACi-induced transformed cell death. These findings support the concept that Chk1 has an important role in protecting normal cells from HDACi-induced cell death. Both normal and transformed cells cultured with vorinostat showed chromosomal abnormalities that are consistent with our previous observation that vorinostat induced DNA DSBs in normal and transformed cells (10). HFS, but not LNCaP, recovered from the HDACi-induced chromosome abnormalities on removal of the inhibitor both by the criteria of restoration of normal mitosis and cell growth.

Vorinostat and romidepsin have been approved by the FDA for the treatment of cutaneous T-cell lymphoma (3–5). These HDACi, as well as a number of others, are in clinical trials that are evaluating possible efficacy in the therapy of hematologic malignancies and solid tumors (1–7). HDACi are being evaluated in combination therapy with various anticancer drugs (1). Inhibitors of Chk1, UCN-01, AZD7762, and CHIR-124, have been evaluated in preclinical and clinical trials in combination with anticancer agents (18–26).
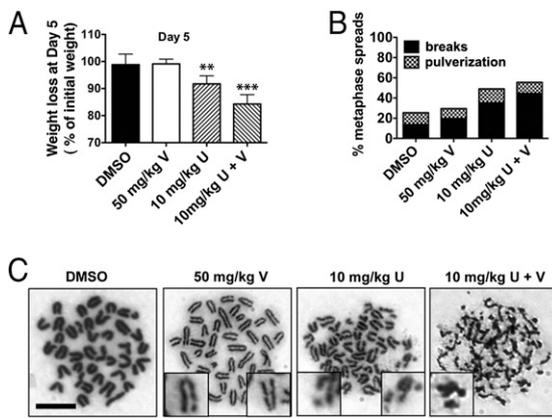
Fig. 5. Effect of vorinostat, UCN-01, or a combination of inhibitors administered to normal mice. (*A*) Average of mice body weight (*n* = 5) on day 5 as a percentage of initial body weight. B6D2F1 mice were injected with 50 mg/kg vorinostat (V), 10 mg/kg UCN-01 (U), or both inhibitors (V + U) for 5 d. Data are represented as mean ± SD. **P < 0.01, ***P < 0.001. *P* value was derived from two-way ANOVA. (*B*) Representative images of mitotic chromosomes of bone marrow cells harvested on day 3 from mice receiving indicated drugs: 50 mg/kg vorinostat (V), 10 mg/kg UCN-01 (U), vorinostat plus UCN-01 (V + U). (Scale bar, 10 μm.) (*C*) Percentage of metaphase spreads with chromosome breaks or pulverized aberrations (*n* > 160 cells) in cells from mice receiving indicated drugs.

The present study is unique in evaluating the effect of Chk1 inhibitor and a DNA damaging agent in normal cells, both in vitro and in vivo. Our finding that Chk1 is essential in preventing HDACi-induced normal cell death indicates that developing combination therapeutic strategies with DNA damaging agents and Chk1 inhibitor may be associated with significant toxicity for normal cells. These findings show that an intact Chk1 plays an important role in the relative resistance of normal cells to HDACi-induced cell death.

Materials and Methods

Cell Lines, Reagents, and Antibodies. HFS cells were purchased from Yale Skin Diseases Research Center Core. A549 cells and LNCaP cells were purchased from American Type Culture Collection and cultured per directions of the supplier. Vorinostat was synthesized as previously reported (30) and was dissolved in DMSO. UCN-01 was purchased from Sigma and was dissolved in 2% sodium citrate (pH 3.5). AZD7762 and CHIR-124 were purchased from Axon Medchem. Entinostat (MS-275) was purchased from Selleck Chemicals. Romidepsin (depsipeptide) was gifted by the National Cancer Institute, Bethesda, MD. Antibodies used were: antiphophorylated Ser-139 histone H2AX and phophorylated Ser-10 histone H3 (Abcam), antiacetylated lysine histone H3 and total histone H3 (Active Motif), anti-Chk1 (Abcam), anti-Chk2 (Millipore), and anti-GAPDH (Thermo Scientific).

Cell Growth and Viability. Each cell culture was performed in triplicate and cell growth and viability performed as described (10). Graphs were constructed using Prism 5 (GraphPad). Data were expressed as mean ± SD.

Immunoblotting Analysis. Cells were collected, washed with ice-cold PBS, and lysed with RIPA cell lysis buffer, and 40 μg of whole cell lysate was resolved by 4–12% Bis-Tris gels (Invitrogen), transferred by semidry transfer iBlot system (Invitrogen), and probed as previously described (10). Graphs for quantifying immunoblot bands were prepared by using TINA 2.0 software (Raytest).

Histone Extraction. Cells 1×10^6 were washed with PBS and lysed with 50 μL histone lysis buffer [10 mM Tris-Cl (pH 6.5), 10 mM $MgCl_2$, 25 mM KCl, 1% Triton X-100, 8.6% sucrose] containing protease inhibitor mixture. After centrifuge at $1,000 \times g$ for 5 min at 4 °C, supernatants were kept for analysis of levels of acetylated tubulin. The pellets were gently resuspended in TE buffer [10 mM Tris-Cl (pH 7.4), 13 mM EDTA], and then centrifuged for 5 min at $600 \times g$ at 4 °C. The pellets were resuspended in ice-cold 0.4 N H_2SO_4, incubated on ice for 1 h, and vortexed 10 s every 15 min during the incubation. Samples were centrifuged for 10 min at $10,000 \times g$ at 4 °C. The supernatants were incubated with ice-cold acetone for at least 1 h at −20 °C. The histone pellets were obtained by centrifugation for 10 min at $10,000 \times g$ at 4 °C. After drying the pellet, histones were resolved in distilled water. A total of 1 μg of histone was used for immunoblot analysis.

RNA Interference. shRNA lentiviral particles targeting Chk1 mRNA (NM_001274) at 7.4×10^6 TU/mL and nontargeting "scramble" shRNA control particles (SHC002V) at 1.1×10^7 TU/mL were purchased from Sigma-Aldrich and transfected according to the manufacturer's instructions using polybrene (Millipore). The 21-nt sequence corresponding to Chk1 mRNA for Chk1 knockdown is 5′-CGCAGTGAAGATTGTAGATAT-3′. For each shRNA, 5×10^5 cells were infected at a multiplicity of infection of two.

Chk1 and Chk2 Kinase Assay. Chk1 and Chk2 kinase assay were done using the K-Lisa kit (Calbiotech). A total of 1 mg of whole cell lysate was used to immunoprecipitate Chk1 or Chk2 by using anti-Chk1 or Chk2 (EMD Chemicals) antibody. K-Lisa assay was performed as previously described (31).

Neutral Comet Assay. HFS or LNCaP cells were seeded at 2.5×10^5 cells/mL in a 6-well plate 24 h before treatment with vorinostat, UCN-01, or a combination of vorinostat and UCN-01. After 24 h, cells were trypsinized, harvested by centrifugation, and resuspended in PBS. Cell counts were then normalized to 1×10^5 cells/mL. Suspended cells (50 μL) were then mixed with 500 μL comet LMAgarose (Trevigen). The agarose-cell mixture was then dropped onto slides and allowed to solidify at 4 °C in the dark for 30 min before immersion in comet assay lysis solution (Trevigen) at 4 °C in the dark for 30 min. Excess buffer was then removed and slides were submerged in 1× TBE buffer [Tris base 108 g, boric acid 55 g, EDTA (disidoum salt) 9.3 g dissolved in 1 L of dH_2O] at room temperature in the dark for 5 min. When performed in neutral electrophoresis buffer, the comet assay measures relative levels of DNA double strand break fragmentation. Slides were then washed twice by immersion in 1× TBE buffer before electrophoresis at 33 V for 15 min. Slides were then fixed in 70% ethanol for 5 min. Following air drying of the agarose, slides were stained with SYBR green dye (Invitrogen) and images were collected with a 10× and 40× objective lens. Comet tail length and olive tail moment were then assessed using COMETscore.v1.5 image processing software as described by the manufacturer with greater than 200 cells analyzed.

Metaphase Spread. Cells were incubated with 0.02 μg/mL colcemid at 37 °C for 2–4 h. Cells were collected by trypsinization, resuspended in 0.075 M KCl hypotonic solution, and incubated for 30 min at 37 °C. For mitotic spreads from bone marrow cells, bone marrow was washed with PBS three times, incubated with colcemid in RPMI for 30 min, and incubated with 0.075 M KCl hypotonic solution for 30 min at 37 °C. Fixative solution (methanol:glacial acetate = 3:1) was added slowly into swollen cells. After centrifugation at $100 \times g$ for 5 min, cells were resuspended in 10 mL fixative solution. Cells were washed several times with fixative, collected in 1 mL of fixative solution, and spread on microscope slides, humidified with water steam. Chromosomes were stained with Giemsa solution (Sigma), mounted with permount, and visualized by using an Olympus microscope and Zeiss Mirax slide scanner. The image analysis was done using ImageJ (National Institutes of Health), Panoramic Viewer (3DHISTECH), and Photoshop CS3 (Adobe) software.

Administration of Vorinostat and UCN-01 for Toxicity Test in Vivo. UCN-01 was dissolved in 2% sodium citrate (pH 3.5) and administered to B6D2F1 6- to 8-wk-old male mice. Each group of mice received 50 mg/kg vorinostat, UCN-01 (5 mg/kg, 10 mg/kg, or 15 mg/kg), or vehicle daily by i.p. injection for 5 d. The injection volume was kept constant at 1 μL/g body weight. The mice were weighed daily during the experimental period to assess toxicity of the treatments and clinical signs were observed. At day 3 after injection, spleen and bone marrow were harvested from one mouse of each group and were prepared for metaphase spreads. At 5 d after the last drug administration, all mice were killed by carbon dioxide inhalation. One animal from each dose group was submitted to an animal pathologist at the Research Animal Resource Center of Cornell University Medical College and Memorial Sloan-Kettering Cancer Center for a complete tissue necropsy and blood cell analysis.

Statistical Analyses. Data are expressed as mean ± SD derived minimally from three independent experiments. Statistical significance was calculated by using the two-tailed Student's *t* test or two-way ANOVA test.

CELL BIOLOGY

1. Ma X, Ezzeldin HH, Diasio RB (2009) Histone deacetylase inhibitors: Current status and overview of recent clinical trials. *Drugs* 69:1911–1934.
2. Marks PA, Xu WS (2009) Histone deacetylase inhibitors: Potential in cancer therapy. *J Cell Biochem* 107:600–608.
3. Marks PA, Breslow R (2007) Dimethyl sulfoxide to vorinostat: Development of this histone deacetylase inhibitor as an anticancer drug. *Nat Biotechnol* 25:84–90.
4. Duvic M, Vu J (2007) Vorinostat: A new oral histone deacetylase inhibitor approved for cutaneous T-cell lymphoma. *Expert Opin Investig Drugs* 16:1111–1120.
5. Grant C, et al. (2010) Romidepsin: A new therapy for cutaneous T-cell lymphoma and a potential therapy for solid tumors. *Expert Rev Anticancer Ther* 10:997–1008.
6. Mercurio C, Minucci S, Pelicci PG (2010) Histone deacetylases and epigenetic therapies of hematological malignancies. *Pharmacol Res* 62:18–34.
7. Kelly WK, et al. (2005) Phase I study of an oral histone deacetylase inhibitor, suberoylanilide hydroxamic acid, in patients with advanced cancer. *J Clin Oncol* 23:3923–3931.
8. Choudhary C, et al. (2009) Lysine acetylation targets protein complexes and co-regulates major cellular functions. *Science* 325:834–840.
9. Ungerstedt JS, et al. (2005) Role of thioredoxin in the response of normal and transformed cells to histone deacetylase inhibitors. *Proc Natl Acad Sci USA* 102:673–678.
10. Lee JH, Choy ML, Ngo L, Foster SS, Marks PA (2010) Histone deacetylase inhibitor induces DNA damage, which normal but not transformed cells can repair. *Proc Natl Acad Sci USA* 107:14639–14644.
11. Kondo S, Perrimon N (2011) A genome-wide RNAi screen identifies core components of the G_2-M DNA damage checkpoint. *Sci Signal* 4:rs1.
12. Chen Z, et al. (2003) Human Chk1 expression is dispensable for somatic cell death and critical for sustaining G2 DNA damage checkpoint. *Mol Cancer Ther* 2:543–548.
13. Bucher N, Britten CD (2008) G2 checkpoint abrogation and checkpoint kinase-1 targeting in the treatment of cancer. *Br J Cancer* 98:523–528.
14. Liu Q, et al. (2000) Chk1 is an essential kinase that is regulated by Atr and required for the G(2)/M DNA damage checkpoint. *Genes Dev* 14:1448–1459.
15. Löbrich M, Jeggo PA (2007) The impact of a negligent G2/M checkpoint on genomic instability and cancer induction. *Nat Rev Cancer* 7:861–869.
16. Hartwell L (1992) Defects in a cell cycle checkpoint may be responsible for the genomic instability of cancer cells. *Cell* 71:543–546.
17. Yamauchi T, Keating MJ, Plunkett W (2002) UCN-01 (7-hydroxystaurosporine) inhibits DNA repair and increases cytotoxicity in normal lymphocytes and chronic lymphocytic leukemia lymphocytes. *Mol Cancer Ther* 1:287–294.
18. Carrassa L, Damia G (2011) Unleashing Chk1 in cancer therapy. *Cell Cycle* 10:2121–2128.
19. Zabludoff SD, et al. (2008) AZD7762, a novel checkpoint kinase inhibitor, drives checkpoint abrogation and potentiates DNA-targeted therapies. *Mol Cancer Ther* 7:2955–2966.
20. Tse AN, et al. (2007) CHIR-124, a novel potent inhibitor of Chk1, potentiates the cytotoxicity of topoisomerase I poisons in vitro and in vivo. *Clin Cancer Res* 13:591–602.
21. Xu H, et al. (2010) Checkpoint kinase inhibitor synergizes with DNA-damaging agents in G(1) checkpoint-defective neuroblastoma. *Int J Cancer* 129:1953–1962.
22. Sausville EA, et al. (2001) Phase I trial of 72-hour continuous infusion UCN-01 in patients with refractory neoplasms. *J Clin Oncol* 19:2319–2333.
23. Kortmansky J, et al. (2005) Phase I trial of the cyclin-dependent kinase inhibitor and protein kinase C inhibitor 7-hydroxystaurosporine in combination with Fluorouracil in patients with advanced solid tumors. *J Clin Oncol* 23:1875–1884.
24. Hotte SJ, et al. (2006) Phase I trial of UCN-01 in combination with topotecan in patients with advanced solid cancers: A Princess Margaret Hospital Phase II Consortium study. *Ann Oncol* 17:334–340.
25. Kummar S, et al. (2010) A phase I trial of UCN-01 and prednisone in patients with refractory solid tumors and lymphomas. *Cancer Chemother Pharmacol* 65:383–389.
26. Cheng H, Merika E, Syrigos KN, Saif MW (2011) Novel agents for the treatment of pancreatic adenocarcinoma. Highlights from the "2011 ASCO Annual Meeting". Chicago, IL, USA; June 3-7, 2011. *JOP* 12:334–338.
27. Bradner JE, et al. (2010) Chemical phylogenetics of histone deacetylases. *Nat Chem Biol* 6:238–243.
28. Xu W, Ngo L, Perez G, Dokmanovic M, Marks PA (2006) Intrinsic apoptotic and thioredoxin pathways in human prostate cancer cell response to histone deacetylase inhibitor. *Proc Natl Acad Sci USA* 103:15540–15545.
29. Butler LM, et al. (2002) The histone deacetylase inhibitor SAHA arrests cancer cell growth, up-regulates thioredoxin-binding protein-2, and down-regulates thioredoxin. *Proc Natl Acad Sci USA* 99:11700–11705.
30. Richon VM, et al. (1998) A class of hybrid polar inducers of transformed cell differentiation inhibits histone deacetylases. *Proc Natl Acad Sci USA* 95:3003–3007.
31. Jayachandran G, Ueda K, Wang B, Roth JA, Ji L (2010) NPRL2 sensitizes human non-small cell lung cancer (NSCLC) cells to cisplatin treatment by regulating key components in the DNA repair pathway. *PLoS ONE* 5:e11994.